Proteomic and metabolomic profiling of Valencia orange fruit after natural frost exposure.

Journal:	*Physiologia Plantarum*
Manuscript ID:	PPL-2013-00587
Manuscript Type:	Regular manuscript - Biochemistry and metabolism
Date Submitted by the Author:	29-Nov-2013
Complete List of Authors:	Perotti, Valeria; Universidad Nacional de Rosario, CEFOBI Moreno, Alejandra; CEFOBI, Trípodi, Karina; Universidad Nacional de Rosario, CEFOBI Meier, Guillermo; INTA, EEA Concordia Bello, Fernando; INTA, EEA Concordia Cocco, Mariángeles; INTA, EEA Concordia Vázquez, Daniel; INTA, EEA Concordia Anderson, Catalina; INTA, EEA Concordia Podestá, Florencio; Universidad Nacional de Rosario, CEFOBI
Key Words:	citrus fruit, cold stress, carbohydrate metabolism, secondary metabolism, proteomics

Title: Proteomic and metabolomic profiling of Valencia orange fruit after natural frost exposure.

Authors: Valeria E. Perotti[a], Alejandra S. Moreno[a], Karina E.J. Trípodi[a], Guillermo Meier[b], Fernando Bello[b], Mariángeles Cocco[b], Daniel Vázquez[b], Catalina Anderson[b] and Florencio E. Podestá[a]

[a]Centro de Estudios Fotosintéticos y Bioquímicos, CONICET, and Facultad de Ciencias Bioquímicas y Farmacéuticas, Universidad Nacional de Rosario, Suipacha 531, 2000 Rosario, Argentina.

[b]Estación Experimental Agropecuaria Concordia (INTA), Estación Yuquerí, Ruta Provincial 22 y vías del Ferrocarril, 3200 Concordia, entre Ríos, Argentina.

Corresponding author:
Dr. Florencio E. Podestá
CEFOBI
Suipacha 531
2000 Rosario
Argentina
Phone & Fax: 54 341 4371955
podesta@cefobi-conicet.gov.ar

Abstract

The aim of this study was to evaluate the response of orange fruit (*Citrus sinensis* var. Valencia late) to freezing stress *in planta*, both immediately after the natural event and after a week, in order to understand the biochemical and molecular basis of the changes that later derive in internal and external damage symptoms. Using two-dimensional differential gel electrophoresis to analyze exposed and non-exposed fruit, 27 differential protein spots were detected in juice sacs and flavedo, among all comparisons made. Also, primary and secondary metabolites relative contents were analyzed in both tissues by GC-MS and LC-MS, respectively. Proteins and compounds involved in regulatory functions, iron metabolism, oxidative damage and carbohydrate metabolism were the most affected. Interestingly, three glycolytic enzymes were induced by cold, and there was an increase in fermentation products (volatiles); all of that suggests that more energy generation might be required from glycolysis to counter the cold stress. Moreover, a notable increase in sugar levels was observed after frost, but it was not at the expense of organic acids utilization. Consequently, these results suggest a probable redistribution of photoassimilates in the frost-exposed plants, tending to restore the homeostasis altered by that severe type of stress. Isosinensetin was the most cold-sensitive secondary metabolite, since it could not be detected at all after the frost, constituting a possible tool to early diagnose freezing damage.

Abbreviations

ADH, alcohol dehydrogenase; ADK, adenosine kinase; C fruit, control fruit; 2D-DIGE, two-dimensional differential gel electrophoresis; DTT, dithiothreitol; EDTA, ethylenediaminetetraacetic acid; FE fruit, frost-exposed fruit; FE+7d fruit, frost-exposed fruit a week after the frost; GC-MS, gas chromatography-mass spectrometry; IEF, electrofocusing; IFR, isoflavone reductase; IPG, immobilized pH gradient; LC-MS, liquid chromatography-mass spectrometry; LDH, lactate dehydrogenase; MDH, NAD-malate dehydrogenase; ME, NADP-malic enzyme; PDC, pyruvate decarboxylase; PEPC, phosphoenolpyruvate carboxylase; PEPCK, phosphoenolpyruvate carboxykinase; PFP_{α}, alpha subunit of pyrophosphate-dependent phosphofructokinase; PFP_{β}, beta subunit of pyrophosphate-dependent phosphofructokinase; PK, pyruvate kinase; PMF, polymethoxylated flavone; PMSF, phenylmethyl sulfonyl fluoride; QRT-PCR, quantitative real-time PCR; ROS, reactive oxygen species; SDS-PAGE, sodium dodecyl sulfate-polyacrylamide gel electrophoresis; TEMED, tetramethyl ethylene diamine.

Introduction

Exposure to frost can derive in many alterations in the vegetative parts and fruit of higher plants, being a major risk factor for the production of citrus fruit in subtropical climates (Purvis 1990). In the case of late-ripening varieties, like Valencia late, frosts can irreversibly arrest the evolution of the maturity index.

The severity of the damage depends on the frost characteristics (minimum temperature and duration), as well as plant-related factors (variety and rootstock, age, health status) and the environmental conditions around the event. Citrus fruits are frozen below -2 ºC, with a minimum frost duration of 6 hours. With lower temperatures, the time needed to produce damage is shorter.

Freeze damage is mostly due to deterioration of the membrane structure, which in turn causes loss of cellular content and a marked dehydration process (Thomashow 1999). Alterations in the fluidity and integrity of membranes directly affect the metabolic processes that are linked to these structures, as respiration or photosynthesis. This is almost always accompanied by generation of reactive oxygen species (ROS) that contribute to membrane destabilization and trigger the antioxidant defense pathways (Sala 1998; Suzuki and Mittler 2006).

Although the cold response of citrus has been intensively studied, most studies were carried out in fruits during postharvest storage. Even more, the few works dedicated to investigate the physiological changes induced by chilling *in planta* have focused in vegetative rather than reproductive organs.

In a previous work, the carbohydrate metabolism and fruit quality were assessed in frost-exposed Valencia orange fruit. Summarily, we found that fruit exposed to natural frost exhibited notorious changes at the level of the respiratory metabolism, with a notable metabolic switch toward a fermentative stage, resulting in fruit of lower quality. Furthermore, it was possible to confirm the involvement of oxidative stress in freeze injury of citrus fruit *in planta* (Falcone Ferreyra et al. 2006).

Proteomics, combined with metabolomics, has proved to be a powerful tool to analyze biochemical pathways and the complex response mechanisms of plants to various abiotic stresses (Ali and Komatsu 2006; Hajheidari et al. 2007; Shi et al. 2008). Therefore, the aim of this study was to broaden our initial characterization of the general changes taking place after a natural frost in orange fruit (Citrus sinensis [L.] Osbeck var. Valencia late). Comparative analysis of both fruit endocarp and epicarp proteome using two-dimensional differential gel electrophoresis (2D-DIGE) was complemented through the evaluation of levels of metabolites such as sugars, organic acids, alcohols, phenylpropanoids and flavonoids. Also, the levels of some mRNA were measured by qRT-PCR.

Materials and methods

Plant material

Assays were conducted with orange fruit [*C. sinensis* (L.) Osbeck] cv 'Valencia Late' grown in the Estación Experimental Agropecuaria INTA, Concordia, Entre Ríos, Argentina, during 2011. Fruits were harvested on July 1st, 4th and 11th, dates corresponding to the period before the frost (control: C), immediately after the frost (Frost-Exposed: FE) and a week after the frost (FE+7d), respectively. The temperature evolution along this period of time can be observed in Supplementary Figure 1. Immediately after harvest, fruit were manually selected for uniformity of colour and the flavedo (epicarp) and juice vesicle tissue (endocarp) were frozen in liquid nitrogen and stored at -80 ºC for further experiments.

Measurement of chemical and internal quality parameters

Control and frost-exposed fruit were squeezed, and the resulting juices were used for the following determinations. Five fruit were used per replication (three replication samples). The total soluble solid content in the juice was determined with a digital refractometer (expressed as ºBrix), and the titratable acidity was measured by titrating with 0.1 N NaOH to pH 8.2. The results are expressed as percentage of citric acid because this is the predominant organic acid in citrus. The maturity index was evaluated via the total soluble solids: titratable acidity ratio.

Ethanol and acetaldehyde content in juice were determined by gas chromatography analysis of juice headspace using a gas chromatograph (Shimadzu Mod. GC17A; Shimadzu Corp., Kyoto, Japan) with a Supelco Omegawax 250 column (30 m x 0.25 mm internal diameter) (Supelco, Bellefonte, PA).

Protein extraction for 2D Electrophoresis

These experiments were carried out in both endocarp and epicarp tissue. Approximately 2 g of endocarp material or 0.5 g of epicarp material were ground in liquid nitrogen using a ceramic mortar and pestle, sand and PVPP. Then, the material was transferred to a SS34 tube containing 2.5 volumes of extraction buffer (100 mM Tris-HCl, pH 8.8, 2% (w/v) SDS, 0.4% (v/v) β-mercaptoethanol, 10 mM EDTA, 1 mM PMSF, 0.9 M sucrose), and 5 volumes of ice-cold Tris-HCl, pH 8.8-saturated phenol, and then agitated at 4 ºC for 30 min. The aqueous phases were back-extracted with extraction media and phenol by vortexing. Tubes were centrifuged at 5000 g for 15 min at 4 ºC and the phenolic phases were transferred to a new tube, leaving the interface intact. Proteins were precipitated with 5 volumes of cold 0.1 M ammonium acetate in methanol at -20 ºC overnight. The samples were collected by centrifugation at 20 000 g at 4 ºC for 20 min. Next, the pellet was washed with 1.5 ml of cold ammonium acetate/methanol and twice with cold 80% (v/v) acetone. A final wash used 1.5 ml of cold 70% (v/v) ethanol. The pellet was resuspended in 2D-DIGE buffer (30 mM Tris-HCl, pH 8.5, 7 M urea, 2 M thiourea, 4% CHAPS) and disrupted in an MSE sonicator by applying 3 x 5 s pulses at 20% power, with 1 min intervals, maintaining the sample on a water-ice bath.

The differential proteome of citrus under cold stress conditions was assessed by comparing frost-exposed fruit (FE and FE+7d) with control samples (C). Three fruit were used per each sample; four replication samples were used.

Protein quantitation

Protein concentration was determined in crude extracts by the method of Bradford using the Bio-Rad protein assay reagent (Bio-Rad, Hercules, CA, USA) and bovine serum albumin as standard.

Protein labelling with dyes

In all experiments, proteins were labelled with Alexa 610 (excitation, 610 nm; emission peak, 628 nm) or Alexa 532 (excitation, 532 nm; emission peak, 554 nm) after adjusting the pH to 8.5 using the supplier's instructions (Molecular Probes Inc. and Invitrogen Ltd). Proteins were labelled at the ratio of 100 µg of protein: 20 nmol of Alexa protein minimal labelling dye in dimethylformamide. After vortexing, samples were incubated for at least 2 h on ice. The reaction was quenched by addition of 1 µl of 1 mM lysine and 20 mM DTT, and 4% (v/v) of isoelectric focusing (IEF) buffers pH 3-10 or 5-8 was added (Amersham Biosciences).

2D-Electrophoresis separation and protein visualization

A 100 µg aliquot of Alexa 532-labelled sample was mixed with 100 µg of Alexa 610-labelled protein prior to 2D gel electrophoresis. A Protean IEF Cell instrument (Bio-Rad, Hercules, CA, USA) was used for IEF with pre-cast immobilized pH gradient (IPG) strips (pH 4–7, linear gradient, 21 cm, Bio-Rad, Hercules, CA, USA). Samples of 450 µl containing the labelled proteins were loaded by in-gel rehydration. The strips were subjected to IEF using the following program: 12 h at 50 V; 1 h at 500 V; 1 h at 1000 V and 8000 V until a final voltage of 68000 V was reached. The strips were equilibrated for the second dimension separation under continuous shaking in SDS equilibration buffer (375 mM Tris-HCl, pH 8.0, 20% glycerol, 2% SDS, and 6 M urea), first with buffer containing 130 mM DTT for 15 min and afterwards with buffer containing 135 mM iodoacetamide for 15 min. The strips were washed briefly with running buffer, then loaded on top of a prepared SDS-PAGE Laemmli gel cast with 15% (w/v) acrylamide (21 x 16 cm), and covered with 0.5% (w/v) agarose. Proteins were separated at 1 W per gel for 12-15 h at 15 ºC using a Ettan Daltsix Electrophoresis System (GE Healthcare), and the gels were scanned using a BioChemi System UVP BioImaging System, employing differential filters for each dye. Data were saved in tiff format. In order to obtain biological replicates, each samples comparison was run in at least three gels using different protein preparations from different fruit. To excise samples for mass spectrometric analysis, a preparative gel loaded with 1 mg of protein was run and stained with CBB R-350 (Amersham Pharmacia Biotech AB, Uppsala, Sweden) in methanol:H_2O:acetic acid (3:6:1).

Gel image analysis

Images were analyzed using Image Master 2D-Platinum (GE Healthcare) using the protocol described in Casati et al. (2006). When necessary, spots were manually edited. A normalization procedure was used to allow for variation in total protein loading onto the gel. Total spot volume was calculated, and each spot was assigned a normalized spot volume as a proportion of this total value. Normalized spot volumes were compared between Alexa 532- and Alexa 610-labelled samples on each gel. Different thresholds were then applied to identify the proteins with a statistically significant 1.5-fold difference in normalized spot volume ($P < 0.05$) (Casati et al. 2005).

In-gel digestion and mass spectrometric analysis

Selected protein spots from the 2D-Electrophoresis gel were manually excised, transferred to 1.5 ml microcentrifuge tubes and sent to the facilities provided by the CEBIQUIEM (Facultad de Ciencias Exactas y Naturales, Universidad de Buenos Aires, Argentina) for further analyses. Spots were subjected to in-gel digestion (donatello.ucsf.edu/ingel.html) with trypsin according to Casati et al. (2006). The mass spectrometric data were obtained using a MALDI-TOF-TOF spectrometer, Ultraflex II (Bruker). Peptide ions were analyzed by the data-dependent method as follows: (1) full MS scan (mass-to charge ratio 800-3000) and (2) MSMS of the major ions. See Supplementary Table 1.

Database search and protein identification

MSMS data were used to perform protein identifications by searching in, at first term, a non-redundant protein sequence database (NCBInr) using MASCOT (www.matrixscience.com, Perkins et al., 1999). The following parameters were used for database searches: taxonomy, *Viridiplantae* (green plants; release December 2008); cleavage specificity, trypsin with 0 or 1 missed cleavage allowed; mass tolerance of 1.2 Da for the precursor ions and a tolerance of 0.7 Da for the fragment ions; allowed modifications, Cys carbamidomethyl (fixed), oxidation of Met (variable).

Only candidates that appeared at the top of the list were considered positive identifications. Peptides were considered as matches if they were classified as 'significant' (i.e. $P < 0.05$, which with our search parameters equals a MOWSE score of >40).

Alternatively, MSMS data was used to perform spot identification by MASCOT software against EST-viridiplantae database. The parameters for these searches and identification criteria were the same as those for the previous search (Perotti et al. 2011). Identified ESTs translated in one of the six open reading frames (ORF) were compared for similarity via BLASTx (http://blast.ncbi.nlm.nih.gov/Blast.cgi). Only the BLASTx matches with E-values$\leq 10^{-30}$ were selected.

Protein functional classification was done according to the classification of the Munich Information Center for Protein Sequences (MIPS, http://mips.gsf.de). See Supplementary Table 2.

Crude extract preparation for GC-MS metabolite analysis

Six hundred mg of flavedo or juice sacs taken from at least six independent fruit were powdered with mortar and pestle in presence of liquid nitrogen. The powder was then transferred to glass tubes and 8.4 ml of cold methanol (-20 ºC) were added. After shaking with vortex, 90 µg of ribitol were added. This latter was used as an inner standard, for the appropriate relative quantification of metabolites. The extract thus obtained was distributed in 6 new glass tubes which were incubated at 70 ºC for 15 min, with periodic agitation. Afterwards, 750 µl of chloroform were incorporated to each tube, and these were incubated at 37 ºC for 5 min. Next, 1.5 ml of water were added and extracts were centrifuged in a refrigerated Sorvall RC-5B microcentrifuge for 15 min at 2200 g. Finally, 450 µl of the polar phase were transferred to Eppendorf tubes and dried in a vacuum centrifuge (CentriVap, Labconco) until complete evaporation, leaving a coloured pellet. Samples were stored at -80 ºC until derivatization.

Sample derivatization and chromatography

Samples were thawed and, dried in a vacuum centrifuge for another 30 min to assure no liquid remaining was present. Afterwards, 40 µl of 20 mg/ml methoxyamine in pyridine were added. Tubes were vigorously shaken and incubated at 37 ºC for 90 min. Finally, 70 µl of N-methyl-N-trimethylsylil-trifluoroacetamide (MSTFA) were incorporated to each tube and incubated at 37 ºC for 30 min.

GC-MS analysis was performed using an autosystem XL Gas Chromatograph and a Turbo Mass Spectrometer (Perkin Elmer). One microliter split injection (split ratio 1:40) was injected at 280 ºC. The capillary column used was a VF-5 ms column (Varian, Darmstadt, Germany) with the following dimensions: 30 m × 0.25 mm inner diameter and a 0.25-µm film with helium as carrier gas with constant flow at 1 ml/min. The temperature program was 5 min at 70 ºC, 5 min ramp to 310 ºC, and final heating for 2 min at 310 ºC. The transfer line to the MS was set to 280 ºC. Spectra were monitored in the mass range m/z = 70–600. Tuning and all other settings were according to manufacturer's recommendations.

Chromatograms were acquired with TurboMass 4.1 software (Perkin Elmer). The NIST98mass spectral search program1 (National Institute of Standards and Technology, Gaithersburg, MD, USA) was the software platform. The MS and retention time index were compared with the collection of the Golm Metabolome Database (gmd.mpimp-golm.mpg.de/). MS matching was manually supervised and matches accepted with thresholds of match >650 (with maximum match equal to 1000) and retention index deviation <1.0%. Peak heights were normalized using the amount of the sample fresh weight and ribitol for internal standardization.

Determination of phenolic compounds by HPLC-MS

Phenolic compounds from flavedo of citrus fruits were analyzed as described in Ballester et al. (2010) with slight modifications. HPLC-MS analysis was performed using an Agilent 1200 HPLC system,

coupled to a G1314C VWD UV detector and a Bruker micrOTOF-Q II spectrometer (Bruker-Daltonics). Freeze-ground material was extracted with 80% methanol. Samples were separated by reverse phase HPLC in a Zorbax XDB 1.8µ C18 column (50mm×3.0mm, Agilent), using a binary gradient elution of acetonitrile and water (pH 2.5). The flow rate was 0.2 ml min^{-1} and the injection volume 5 µl. Elution was monitored at 280nm. MS settings were as follows: source type, ESI; ion polarity, positive; nebulizer, 1.0 bar; dry heater, 200 ºC; dry gas, 4.0 l/min; capillary, 4500V; end plate offset, 500V; collision cell RF, 150.0 Vpp. The compounds levels were expressed as the area (mAU) of the peak in the chromatogram by gram of fresh weight.

RNA isolation and RT-PCR

Total RNA from different samples of epicarp was isolated from 100 mg of tissue using TRI Reagent (Sigma-Aldrich, St. Louis, MO, USA). The integrity of the RNA was verified by agarose electrophoresis. The quantity and purity of RNA were determined spectrophotometrically. First-strand cDNA was synthesized with M-MLV-reverse transcriptase following the manufacturer's instructions (Promega, Madison, WI, USA) and using oligo(dT) and 2 µg of RNA previously treated with DNase I (Promega).

Quantitative real-time PCR

Relative expression was determined by performing quantitative real-time PCR (QRT-PCR) in an iCycler iQ detection system with the Optical System Software version 3.0a (Bio-Rad), using the intercalation dye SYBR Green I (Invitrogen) as a fluorescent reporter, with 3 mM $MgCl_2$, 1 µM of each primer, and 0.04 U $µl^{-1}$ of Platinum Taq DNA polimerase (Invitrogen). Primers were designed using the PRIMER3 software and taking into consideration the citrus fruit cDNA sequences published in GenBank and *C. sinensis* expressed sequence tag (EST) databases (HarvEST: Citrus) (Table 1). A 4-fold dilution of cDNA obtained as described above was used as template. Cycling parameters were as follows: initial denaturation at 94 ºC for 3 min; 40 cycles of 95 ºC for 15 s, 58 ºC for 15 s and 72 ºC for 20 s; and a final step at 72 ºC for 10 min. Melting curves for each PCR were determined by measuring the decrease of fluorescence with increasing temperature (from 65 ºC to 98 ºC). The specificity of the PCRs was confirmed by melting curve analysis using the appropriate software as well as by agarose gel electrophoresis of the products. The PCR products were purified from the gel and sequenced to verify their identities. Elongation factor 1 was using as reference gene. This analysis was performed in at least three biological replicates and each RNA sample was run in duplicate.

Statistical analysis

Data from the experiments were tested using one-way analysis of variance (ANOVA). Minimum significant differences were calculated by the Bonferroni Test ($\alpha = 0.05$) using the Sigma Stat Package. In some cases, it was not possible to pass the Tests mentioned above, so data were tested

using the non-parametric method Kruskal-Wallis one-way analysis of variance by ranks. Minimum significant differences were calculated by the Tukey Test (or Dunn's Method, if the treatment group sizes were unequal) ($\alpha = 0.05$).

Results

General description of the experiments

In order to characterize the changes occurring after a frost in orange fruits, the fast response (immediately after the episode) and the later response (a week after the episode) were studied in fruits naturally exposed to the first severe frost during the winter of 2011. Supplementary Figure 1 shows the temperature registration during the days before and after this frost. This experimental design allows the evaluation of the evolution of internal changes before the well known symptoms appear.

Evaluation of cold injury by quality parameters

A visual inspection of the three samples (C, FE and FE+7d) (see Materials and Methods) did not reveal any differences, because the freezing damage is manifested only after a longer period of time in this fruit. Similarly, the maturity index was not modified among the samples analyzed (Table 2). However, an immediate increase of volatile compounds was observed, demonstrating alterations in the fruit towards a fermentative metabolism, as was reported previously (Falcone Ferreyra et al. 2006).

Proteomic analysis of cold-stress response in *C. sinensis*

2D-DIGE analysis was carried out in both endocarp and epicarp tissue. Statistical analysis allowed the identification of significant differences in the proteomic profiles. Proteins with a minimum of 1.5-fold differential expression were subjected to mass spectrometry analyses. Following this procedure, 27 differential protein spots were detected in juice sacs and flavedo, among all comparisons made. Figure 1 depicts a representative two-dimensional electrophoresis map showing the spot distribution of proteins from epicarp. The differentially expressed proteins identified by MS analysis are listed in Table 3. The complete list of peptide sequences from identified proteins is shown in Supplementary Table 1.

Among the proteins that increased in abundance under cold stress, spots 2, 11 and 21 were not identified but the other eleven proteins were identified as carboxymethylenebutenolidase (spot 1), isoflavone reductase (spot 3), ferritin (spot 5), fructose bisphosphate aldolase (spot 7), NADH dehydrogenase (spots 12 y 16), phosphoglycerate kinase (spot 14), germin-like protein (spot 17), 2-phospho-D-glycerate hydrolase (spot 18), ATP synthase beta subunit (spot 19) and RuBisCO subunit binding-protein alpha subunit (spot 20). Proteins with a reduced abundance after the frost matched to ferritin (spot 5 again), adenosine kinase (spot 6), 3-isopropylmalate dehydratase (spot 8), nascent polypeptide-associated complex subunit alpha (spot 10), aconitate hydratase (spot 15), HSP 70 protein-like (spot 22), germin-like protein (spot 23), progesterone 5-beta-reductase (spot 26) and RuBisCO large subunit (spot 27). It should be noted that ferritin showed an interesting behavior since this protein could not be detected immediately after the frost but increased markedly a week later.

The identified proteins were classified into functional groups, following the classification of the Munich Information Center for Protein Sequences (MIPS, http://mips.gsf.de). These results are

summarized in Supplementary Table 2. Accordingly, the major category found to be affected was "Metabolism" in both tissues.

Analysis of most abundant metabolites by GC-MS

Organic acids, sugars, alcohols and other compounds were measured in C, FE and FE+7d samples, both in juice sacs and flavedo (Figures 2 and 3, respectively).

Regarding the internal tissue, GC-MS analysis revealed that the most abundant acids (citric and malic acids) did not show any variation, in concordance to the titratable acidity determinations (see Table 2). Other acids exhibited an increase immediately after the frost but then returned to the initial levels, with the exceptions of aspartic, uric and lactic acids, which showed lower values in FE+7d samples and dehydroascorbic acid, which was not affected at all. Sugars levels were notably increased a week after the frost. A similar tendency was observed for myo-inositol and phosphate, while glycerol showed the opposite behavior.

Some similar patterns could be appreciated in flavedo, such as the rise in sugars, myo-inositol and phosphate and the decrease of glycerol and lactic and uric acids in FE+7d samples. On the other hand, organic acids levels showed considerable changes in this tissue, oppositely with the results obtained in juice sacs. Thus, citric, malic and aspartic acids levels were higher in FE+7d samples, while maleic acid levels were undetectable in these samples. It is worth to highlight the marked increase in proline levels, a known compatible solute induced by different types of stress in plants.

Examination of phenylpropanoids alterations in flavedo by LC-MS

The most abundant phenolic compounds in flavedo did not show major changes after frost exposure (Figure 4), with the exception of didymin, which showed a significant increase in FE+7d samples. However, the minor compounds showed marked differences, revealing at least two different patterns: a decrease along the time after frost (sinensetin, tangeretin, heptamethoxyflavone, tetramethyl-O-scutellarein); and an immediate decrease after frost, followed by a recovery a week later (narirutin, nobiletin, chlorogenic acid). It is worth to note that isosinensetin levels were the most cold-sensitive, since this metabolite could not be detected at all after the frost.

Gene expression analysis in flavedo by qRT-PCR

Several enzymes involved in sugar metabolism and some interesting proteins detected in the proteomic assays were analyzed in flavedo by qRT-PCR (Figure 5).

While the transcript levels of malate dehydrogenase (MDH) and phosphoenolpyruvate carboxykinase (PEPCK) increased in samples FE+7d, those of phosphoenolpyruvate carboxylase (PEPC) decreased immediately after frost and were still low a week later. The pyrophosphate-dependent phosphofructokinase (PFP, both subunits) and malic enzyme (ME) transcript levels followed a similar profile: an initial fall, followed by a recovery to the initial values. However, these variations were not

significant. The expression of the fermentative enzymes alcohol dehydrogenase (ADH), pyruvate decarboxylase (PDC) and lactate dehydrogenase (LDH) showed an important induction in FE+7d samples, in general agreement with the observed surge in high volatile compounds production (Table 2), and to previous results (Falcone Ferreyra et al. 2006).

Concerning spots transcript levels, only the spot 26 (progesterone 5-beta-reductase) showed a significant change, which was coincident with the variations observed by 2D-DIGE at protein level.

Discussion

In this report, the biochemical response of Valencia late oranges to a natural frost was investigated using different approaches. The experimental design used in this paper allowed following the progress of this response along the time, before the appearance of visual damage. The information thus gathered could be used for an early evaluation of the degree of compromise of the fruit by a cold spell and to determine the commercial fate of the produce.

Using 2D-DIGE, several proteins whose abundance is modified by frost were found. This analysis was performed both in endocarp and epicarp. The experimental Mr and pI of several of the identified proteins were not exactly equal to the predicted values of matching proteins. This apparent incongruence could be explained by different factors such as expression in a different organism or tissue, or posttranslational modifications (Muccilli et al. 2009; Pan et al. 2009).

Among the differential proteins affected immediately after the frost, it was possible to identify three spots in juice sacs and ten spots in flavedo. When the late response was analyzed, five spots of six were identified in juice sacs and two of three in flavedo.

In parallel, the GC-MS analysis revealed that a large fraction of the metabolites analyzed was significantly changed in at least one of the conditions studied, being flavedo the most affected tissue.

Next, the main alterations in the frost-exposed citrus proteome and the most interesting changes in metabolites content will be discussed, in order to integrate both views.

Carbohydrate metabolism

Metabolism was the main functional category affected upon the conditions studied; in particular, carbohydrates metabolism. This result was observed along the most of the temperature-stress studies in plants, therefore it seems to be a major feature of the cellular reprogramming during temperature stress.

Three glycolytic enzymes were induced by cold: fructose-bisphosphate aldolase, phosphoglycerate kinase and enolase. An enhanced expression of fructose-bisphosphate aldolase in response to saline, cold and water stress in different plant tissues has been previously reported (Abbasi and Komatsu 2004; Hashimoto and Komatsu 2007). A possible reason for up-regulation of aldolases could be a greater ability to synthesize ATP in glycolysis and ethanolic fermentation, processes intensified upon oxidative stress. This hypothesis is consistent with previous findings in frost-exposed endocarp, where freezing temperatures provoked a notable metabolic switch in citrus fruit toward fermentation (Falcone Ferreyra et al. 2006), and is reaffirmed in this study by the higher volatile compounds levels observed after frost (Table2). Similarly to this outcome, phosphoglycerate kinase levels were enhanced by both salt and cold stress in rice leaf, suggesting that this enzyme is an early responsive protein to both adverse conditions (Hashimoto and Komatsu 2007). Additionally, a strong induction of this enzyme in Arabidopsis leaves undergoing cold stress has been observed (Jung et al. 2003). In the

same way, enolase (2-phospho-D-glycerate hydrolase) also showed higher expression levels upon cold stress (Komatsu et al. 2009).

In summary, induction of all of these sugar metabolism-related proteins plus the increase in fermentation products (volatiles) suggested that more energy generation might be required from glycolysis to counter the cold stress, probably by a reduction of mitochondrial functionality.

Sugars levels were remarkably increased a week after the frost, both in endocarp and epicarp. In citrus peel, sugars mediate interconversions between chloroplasts and chromoplasts and can also stimulate changes in chlorophyll, carotenoid, and plastid characters *in vitro* (Koch 1996). Interestingly, many of the nuclear-encoded plastid genes are regulated by sugar levels. Coincidently, in this work, the abundance of some plastid proteins was affected (spots 19, 20 and 27).

Leaves support the reproductive organs by provision of photosynthates, hormones, among other mechanism (Ruiz and Guardiola 1994). In citrus leaves, soluble sugars increase toward midwinter, as an osmotic, cryoprotective measure against cold injury, while the demand of developing fruit is progressively reduced (Yelenosky and Guy 1977).

It is well known that juice sacs increase sugars levels along the maturity at the expense of organic acids degradation. However, the higher sugar amounts observed in FE+7d samples could not be explained in this way, because the major acids did not decrease at all. Since fruit under study is still in stage II, this result could be interpreted as a consequence of a higher provision of sucrose by the vegetative parts combined with a thwarted mitochondrial functionality that could hinder acid conversion or its use by means of respiration. Consequently, our results support the notion that apparent sink strength of the fruit is somehow increased by the frost episode.

Myo-inositol and phosphate showed the same tendency observed for sugars. An increase of myo-inositol could be the result of degradation of inosytol phosphates, such as 1-l-myo-inosytol-1-phosphate (MIP). This metabolite is connected to essential cellular functions, such as phosphorus storage, stress protection, hormonal homoeostasis and cell wall biosynthesis (Downes et al. 2005; Loewus and Murthy 2000). Both myo-inositol and Pi could proceed from MIP degradation. Pi released could be used for increased sugar phosphorylation, since upon an intensified fermentative metabolism, more sugar catabolism will be needed to support ATP synthesis.

In relation to that, an increase in two glycolytic enzymes (PFP and PEPC) that catalyze bypasses to nucleotide-utilizing steps was reported previously in juice sacs of frost-exposed oranges (Falcone Ferreyra et al. 2006). Conversely, the gene expression analysis in the flavedo carried out in this study showed that PEPC transcript decreased immediately after frost and remained low a week later, while PFP (both subunits) did not present any significant change. However, these analyses were performed in different tissues and the contribution of other isoforms cannot be discarded. Moreover, the apparent discrepancy between transcript levels and protein abundances can be explained by several reasons, appropriately discussed by Fernie and Stitt (Fernie and Stitt 2012).

Proteins involved in regulatory functions

Frequently, plants respond to different stress conditions using common regulatory mechanisms that are composed of a series of events involved in stress sensing, signal transduction and gene expression regulation. In our study, some proteins involved in these regulation processes were recognized.

For instance, spot 10 was identified as nascent polypeptide-associated complex (NAC) subunit alpha-like. It can reversibly bind to eukaryotic ribosomes and is probably the first cytosolic protein to contact nascent polypeptide chains emerging from ribosome. In plants, the function of NAC is still unclear. It has been suggested that NAC is involved in protein sorting and translocation. Some evidence proposes that the α-NAC could function as a transcriptional coactivator (Yotov et al. 1998). Our results showed that the protein of α-NAC was down-regulated by cold stress. A similar behavior was observed in rice root by salt stress (Yan et al. 2005).

In addition, the previously mentioned enolase is also present in the nucleus, where, along with other transcription factors such as CBFs/DREB1s, constitutes a fine-tuned transcriptional regulatory circuitry for optimal cellular responses to cold environment (Lee et al. 2002).

Spots 17 and 23 showed opposite variations in flavedo after frost and both proteins belong to a large and highly diverse family of ubiquitous plant proteins called germins. Several of these proteins are glycoproteins associated with the extracellular matrix and involved in the response to various stress conditions. Although their exact participation in these processes remains generally obscure, three classes of functions are starting to be recognized for these proteins: some possess an enzymatic activity (oxalate oxidase or superoxide dismutase); others seem to be structural proteins while some others act as receptors (Bernier and Berna 2001).

Secondary metabolism

The accumulation of secondary metabolites has been reported as a sign of an activated defense mechanism in plants and considered to be important for cell acclimation against stress (Rivero et al. 2001). Therefore, it is reasonable that some proteins involved in these pathways are differentially expressed upon the comparisons made.

For instance, adenosine kinase (ADK) catalyzes the phosphorylation of adenosine to adenosine monophosphate and is involved in the salvage pathways of both adenine (Ade) and adenosine (Ado) and thus is a component of the adenylate metabolic network. Ade and Ado salvage activities are involved in the conversion of cytokinin (CK) bases and ribosides to their corresponding nucleotides. This conversion may be important in regulating the level of this hormone in plant cells (Moffatt et al. 2000). Moreover, the lack of Ado recovering in the ADK-deficient arabidopsis lines resulted in the inhibition of S-adenosyl-Met-dependent transmethylation (Moffatt et al. 2002). Consequently, transmethylation reactions in the metabolism of secondary products would be affected in oranges after frost, given that ADK decreases in endocarp.

On the other hand, carboxymethylenebutenolidase, a protein involved in secondary metabolites biosynthesis, increased immediately after frost. Higher levels of this protein have been observed in barley roots under salinity stress (Witzel et al. 2009). Other general stress-inducible protein found was isoflavone reductase (IFR), an enzyme specific for the biosynthesis of isoflavonoid phytoalexins. Regarding cold stress, IFR was increased by chilling treatment in rice root tissue, suggesting that along with antioxidants, secondary metabolites play a crucial role in cell signaling or maintaining the redox status of cells (Lee et al. 2009). In this special case, higher levels of IFR may be part of a general defense mechanism to ward off cold-exposed tissue from microbial infection or to minimize the damage of an oxidative burst.

Iron metabolism and oxidative damage

Iron is an essential nutrient for plants, where it participates in many electron transfer reactions. Hence it has an important role in respiration and photosynthesis. However, high levels become toxic because it generates oxidative damage via the Fenton reaction. Most of the iron required in eukaryotic cells is consumed by the synthesis of heme and Fe-S centers. These two processes are performed in the mitochondria and need active transport of reduced iron through the inner mitochondrial membrane (Lange et al. 1999) and storage proteins, such as ferritin. Therefore, alterations in mitochondrial membranes caused by freezing conditions could disrupt cellular iron homeostasis, as discussed below.

As was mentioned, ferritin is an iron-binding protein which is proposed to protect plants from oxidative damage induced by a wide range of stresses (Ravet et al. 2009). Notably, an isoform of this family disappeared immediately after the frost episode but reappeared with higher intensity after a week. This result contrast with other observations that report no effect of cold stress in ferritin expression in pear (Xi et al. 2011), and the upregulation in a cold tolerant alpine plant (Zhang et al. 2009). Whether the disappearance really reflects lack of protein or its modification in such a way that it no longer migrates to the same spot is not clear at this time. One aspect that needs to be further investigated is the location of ferritin in citrus fruit, because if ferritin is predominantly mitochondrial and these organelles are seriously affected by frost, then it is not surprising that a complete loss is observed after the episode. Its reemergence after a week may be the consequence of an adaptation to the intense stress situation that frost brings about.

Aconitase (aconitate hydratase), an enzyme of the tricarboxylic acid cycle, and 3-isopropylmalate dehydratase, a protein with strong sequence homology to aconitase, showed lower protein levels by cold stress in epicarp and endocarp, respectively. Accordingly with our results, aconitate hydratase showed enhanced degradation during chilling stress in rice leaves (Yan et al. 2006). This enzyme is exquisitely sensitive to ROS and was shown to be down-regulated by oxidative stress in Arabidopsis (Sweetlove et al. 2002). Meanwhile, 3-isopropylmalate dehydratase would be involved in Leu biosynthesis pathway (Binder et al. 2007). Curiously, proteins belonging to the aconitase family from animal and bacteria are able to switch to RNA-binding proteins called IRPs (Iron-Regulatory

Proteins), playing a key role in the regulation of iron homoeostasis. However, there is no evidence about that this is happening in plants (Arnaud et al. 2007). Future studies are necessary to clear this interesting point.

Cold stress has previously been reported to induce enzymatic changes in the plant respiratory chain, especially in energy dissipating pathways. Lee and collaborators suggested that the mitochondrial protein NADH dehydrogenase would be involved in nuclear gene expression under low-temperature conditions, possibly through reactive oxygen messengers (Lee et al. 2002). It is very interesting that spots 12 and 16 were identified as NADH dehydrogenase components and both showed a higher expression level after frost. Additionally, the lower uric acid levels in both tissues after frost would also be related to ROS, since this acid might act as a precursor for allantoin and allantoate, two ureides recently linked with protecting plants against abiotic stress (Werner and Witte 2011).

Taking to account all the above, alterations in these components could be explained as the first step in a specific regulation to induce the acclimation response, probably directed by ROS.

Photosynthesis

Spots 19 and 20, both induced by frost, were identified as ATP synthase beta subunit and RuBisCO subunit binding-protein alpha subunit, respectively. As in rice seedlings under cold stress (Cui et al. 2005), up-regulation of ATPase subunits may be the sign of an increased effort to obtain more energy from photosynthesis. This makes sense if it is taken into account that mitochondria functionality, as discussed above, may be compromised. Thus, it is reasonable that in flavedo, where there are some chloroplasts, an increased photosynthesis could compensate for a lower mitochondrial ATP-fed biosynthetic activity.

However, spot 27, identified as RuBisCO large subunit, was suppressed 7 days after frost. There are reports that cold stress affects RuBisCO levels, as it was found to be more abundant in chilled tomato (Vega-García et al. 2010). Nevertheless, it was also reported that RuBisCO was down-regulated during cold stress (Hashimoto and Komatsu 2007; Komatsu et al. 1999). It was suggested that upon cold stress, there is either an activation of proteases, which results in degradation of the RuBisCO large subunit, or there is an increase in the production of free radicals, which are known to fragment this polypeptide. Neither hypothesis can be discarded at this time. According to our previous findings, probably both of them are contributing (Falcone Ferreyra et al. 2006).

Spot 22 and 26

These two spots showed a decrease after frost, and deserve a special section because their particular functions.

Spot 22 was identified as a heat shock protein, the expression of which was lower after frost. Stress 70 molecular chaperones are found in all the major subcellular compartments of plant cells, and they are encoded by a multigene family. The expression of the stress 70 molecular chaperones in response to

heat shock is well-known and it appears that low temperature exposure can also stimulate their expression. However, it has been difficult to determine which member(s) of the family are specifically responsive to low temperature. Moreover, some members show a down-regulation upon the restoration of an optimal temperature (Li et al. 1999).

Spot 26 was identified as progesterone 5β-reductase. This enzyme has been proposed to have a key function in the cardenolide-producing branch, forming the required 5β-configured pregnanes. Its activity has been directly correlated with cardenolide biosynthesis (Stuhlemmer and Kreis 1996). Cardenolide is a plant defense toxin which acts as specific inhibitor of animal Na+/K+-ATPase (Wittstock and Gershenzon 2002). Therefore, a rise of this protein could be related to a preventive anti-pathogen response in these more susceptible fruits, much along the same line as the proposal stated above for phytoalexins. Even more, progesterone 5β-reductase mRNA also showed a significant increase in FE+7d flavedo samples (Figure 5). However, there is no evidence about the presence of this compound in citrus. Further investigations are required to gain insight into this interesting finding.

Flavonoids profile alterations

In order to perform a deeper characterization of the most affected tissue, LC-MS were carried out in flavedo samples, focusing in the relative quantification of the main phenolic compounds. Although the role of many phenylpropanoids in plant responses to stressors have been recognized, the details of most of these responses have not been elucidated yet. While most of the flavonoids were found not to be significantly affected in this study, some compounds showed marked differences, revealing at least two different patterns, as described above. The most interesting behaviors were observed for isosinensetin, a polymethoxylated flavone (PMF) only detected in C samples; and didymin, the second most abundant flavanone in *C. sinensis* flavedo, after hesperidin, which increased in FE+7d flavedo.

PMFs content is high in the peel but low in the pulp and juice of the fruit (Goulas and Manganaris 2012; Lafuente et al. 2011) and they play a key role in the defense responses of citrus fruit against pathogens. Oppositely to the other PMFs, isosinensetin did not show any alteration after an elicitor treatment to increase the resistance of oranges to a subsequent pathogen infection (Ballester et al. 2013), suggesting a different physiological role for this particular PMF. It is worth exploring whether the observed response of isonestensin can be used as a tool to detect early damage on FE fruit.

On the other hand, didymin levels increased under the mentioned conditions of that work, confirming its involvement in the induction of natural resistance. Interestingly, a pro-apoptotic property of didymin was reported in non-small-cell lung cancer (Hung et al. 2010); but how didymin works to induce apoptosis and if it has an implication in some plant tissue remain to be elucidated.

Concluding remarks

The natural frost-exposure produces several alterations in the general metabolism of orange fruits, as has been described in the precedent lines. To the best of our knowledge, this is the first report of the

differential proteome in citrus upon freezing conditions *in planta*. What molecular adjustments take place in the whole plant after frost remains to be elucidated. In particular, it would be very interesting to investigate how carbohydrate metabolism is affected in the photosynthetic tissues of these frost-exposed plants to evaluate the redistribution of photoassimilates under this severe type of stress.

Acknowledgements.

This work was made possible by grants PICT 2011-01122 from Agencia Nacional para la Promoción de la Ciencia y Tecnología and PIP 2159 from the Consejo Nacional de Investigaciones Científicas y Técnicas (CONICET). ASM and VEP are Fellows and FEP is a member of the Investigator Career of the same Institution.

Abbasi FM and Komatsu S (2004) A proteomic approach to analyze salt-responsive proteins in rice leaf sheath. *Proteomics* **4**:2072-2081.

Ali GM and Komatsu S (2006) Proteomic Analysis of Rice Leaf Sheath during Drought Stress. *J Proteome Res* **5**:396-403.

Arnaud N, Ravet K, Borlotti A, Touraine B, Boucherez J, Fizames C, Briat J-F, Cellier F and Gaymard F (2007) The iron-responsive element (IRE)/iron-regulatory protein 1 (IRP1)–cytosolic aconitase iron-regulatory switch does not operate in plants. *Biochem J* **405**:523–531.

Ballester A-R, Lafuente MT, Vos RCHd, Bovy AG and González-Candelas L (2013) Citrus phenylpropanoids and defence against pathogens. Part I: Metabolic profiling in elicited fruits. *Food Chem* **136**:178–185.

Ballester AR, Izquierdo A, Lafuente MT and González-Candelas L (2010) Biochemical and molecular characterization of induced resistance against Penicillium digitatum in citrus fruit. *Postharv Biol Technol* **56**:31-38.

Bernier Fo and Berna A (2001) Germins and germin-like proteins: Plant do-all proteins. But what do they do exactly? *Plant Physiol Biochem* **39**:545-554.

Binder S, Knill T and Schuster J (2007) Branched-chain amino acid metabolism in higher plants. *Physiol Plant* **129**:68-78.

Casati P, Zhang X, Burlingame AL and Walbot V (2005) Analysis of Leaf Proteome after UV-B Irradiation in Maize Lines Differing in Sensitivity. *Mol Cell Proteomics* **4**:1673-1685.

Cui S, Huang F, Wang J, Ma X, Cheng Y and Liu J (2005) A proteomic analysis of cold stress responses in rice seedlings. *PROTEOMICS* **5**:3162-3172.

Downes CP, Gray A and Lucocq JM (2005) Probing phosphoinositide functions in signaling and membrane trafficking. *Trends Cell Biol* **15**:259-268.

Falcone Ferreyra ML, Perotti V, Figueroa CM, Garrán S, Anderson PC, Vázquez D, Iglesias AA and Podestá FE (2006) Carbohydrate metabolism and fruit quality are affected in frost-exposed Valencia orange fruit. *Physiol Plant* **128**:224-236.

Fernie AR and Stitt M (2012) On the Discordance of Metabolomics with Proteomics and Transcriptomics: Coping with Increasing Complexity in Logic, Chemistry, and Network Interactions. *Plant Physiol* **158**:1139–1145.

Goulas V and Manganaris GA (2012) Exploring the phytochemical content and the antioxidant potential of Citrus fruits grown in Cyprus. *Food Chem* **131**:39–47.

Hajheidari M, Eivazi A, Buchanan BB, Wong JH, Majidi I and Salekdeh GH (2007) Proteomics Uncovers a Role for Redox in Drought Tolerance in Wheat. *J Proteome Res* **6**:1451-1460.

Hashimoto M and Komatsu S (2007) Proteomic analysis of rice seedlings during cold stress. *PROTEOMICS* **7**:1293-1302.

Hung J-Y, Hsu Y-L, Ko Y-C, Tsai Y-M, Yang C-J, Huang M-S and Kuo P-L (2010) Didymin, a dietary flavonoid glycoside from citrus fruits, induces Fas-mediated apoptotic pathway in human non-small-cell lung cancer cells in vitro and in vivo. *Lung Cancer* **68**:366–374.

Jung S-H, Lee J-Y and Lee D-H (2003) Use of SAGE technology to reveal changes in gene expression in Arabidopsis leaves undergoing cold stress. *Plant Mol Biol* **52**:553-567.

Koch KE (1996) CARBOHYDRATE-MODULATED GENE EXPRESSION IN PLANTS. *Annu Rev Plant Physiol Plant Mol Biol* **47**:509–540.

Komatsu S, Karibe H, Hamada T and Rakwal R (1999) Phosphorylation upon cold stress in rice (Oryza sativa L.) seedlings. *Theor App Genet* **98**:1304-1310.

Komatsu S, Yamada E and Furukawa K (2009) Cold stress changes the concanavalin A-positive glycosylation pattern of proteins expressed in the basal parts of rice leaf sheaths. *Amino Acids* **36**:115-123.

Lafuente MT, Ballester AR, Calejero J, Zacarías L and González-Candelas L (2011) Effect of heat-conditioning treatments on quality and phenolic composition of cold stored 'Fortune' mandarins. *Food Chem* **128**
1080–1086.

Lange H, Kispal G and Lill R (1999) Mechanism of Iron Transport to the Site of Heme Synthesis inside Yeast Mitochondria. *J Biol Chem* **274**:18989-18996.

Lee DG, Ahsan N, Lee SH, Lee JJ, Bahk JD, Kang KY and Lee BH (2009) Chilling stress-induced proteomic changes in rice roots. *J Plant Physiol* **166**:1-11.

Lee H, Guo Y, Ohta M, Xiong L, Stevenson B and Zhu J-K (2002) LOS2, a genetic locus required for cold-responsive gene transcription encodes a bi-functional enolase. *EMBO J* **21**:2692-2702.

Li Q-B, Haskell D and Guy C (1999) Coordinate and non-coordinate expression of the stress 70 family and other molecular chaperones at high and low temperature in spinach and tomato. *Plant Mol Biol* **39**:21-34.

Loewus FA and Murthy PPN (2000) Myo-Inositol metabolism in plants. *Plant Sci* **150**:1-19.

Moffatt BA, Stevens YY, Allen MS, Snider JD, Pereira LA, Todorova MI, Summers PS, Weretilnyk EA, Martin-McCaffrey L and Wagner C (2002) Adenosine Kinase Deficiency Is Associated with Developmental Abnormalities and Reduced Transmethylation. *Plant Physiol* **128**:812-821.

Moffatt BA, Wang L, Allen MS, Stevens YY, Qin W, Snider J and von Schwartzenberg K (2000) Adenosine Kinase of Arabidopsis. Kinetic Properties and Gene Expression. *Plant Physiol* **124**:1775-1785.

Muccilli V, Licciardello C, Fontanini D, Russo MP, Cunsolo V, Saletti R, Reforgiato Recupero G and Foti S (2009) Proteome analysis of Citrus sinensis L. (Osbeck) flesh at ripening time. *J Proteomics* **73**:134-152.

Pan Z, Guan R, Zhu S and Deng X (2009) Proteomic analysis of somatic embryogenesis in Valencia sweet orange (Citrus sinensis Osbeck). *Plant Cell Rep* **28**:281-289.

Perotti VE, Del Vecchio HA, Sansevich A, Meier G, Bello F, Cocco M, Garrán SM, Anderson C, Vázquez D and Podestá FE (2011) Proteomic, metabalomic, and biochemical analysis of heat treated Valencia oranges during storage. *Postharv Biol Technol* **62**:97-114.

Purvis AC (1990) Relation of chilling stress to carbohydrate composition., in *Chilling injuries of horticultural crops* (Wang C ed), CRC Press, Boca Raton, Fl. pp 211-221.

Ravet K, Touraine B, Boucherez J, Briat J-F, Gaymard F and Cellier F (2009) Ferritins control interaction between iron homeostasis and oxidative stress in Arabidopsis. *The Plant Journal* **57**:400-412.

Rivero RM, Ruiz JM, García PC, López-Lefebre LR, Sánchez E and Romero L (2001) Resistance to cold and heat stress: accumulation of phenolic compounds in tomato and watermelon plants. *Plant Science* **160**:315-321.

Ruiz R and Guardiola JL (1994) Carbohydrate and mineral nutrition of orange fruitlets in relation to growth and abscission. *Physiol Plant* **90**:27-36.

Sala JM (1998) Involvement of oxidative stress in chilling injury in cold stored mandarin fruits. *Postharvest Biol Technol* **3**:255-261.

Shi JX, Chen S, Gollop N, Goren R, Goldschmidt EE and Porat R (2008) Effects of anaerobic stress on the proteome of citrus fruit. *Plant Sci* **175**:478-486.

Stuhlemmer U and Kreis W (1996) Cardenolide formation and activity of pregnane-modifying enzymes in cell suspension cultures, shoot cultures and leaves of Digitalis lanata. *Plant Physiol Biochem* **34**:85–91.

Suzuki N and Mittler R (2006) Reactive oxygen species and temperature stresses: A delicate balance between signaling and destruction. *Physiol Plant* **126**:45-51.

Sweetlove LJ, Heazlewood JL, Herald V, Holtzapffel R, Day DA, Leaver CJ and Millar AH (2002) The impact of oxidative stress on Arabidopsis mitochondria. *Plant J* **32**:891-904.

Thomashow MF (1999) Plant cold acclimation: Freezing Tolerance Genes and Regulatory Mechanisms. *Annu Rev Plant Physiol Plant Mol Biol* **50**:571-599.

Vega-García MO, López-Espinoza G, Ontiveros JC, Caro-Corrales JJ, Vargas FD and López-Valenzuela JA (2010) Changes in Protein Expression Associated with Chilling Injury in Tomato Fruit. *J Amer Soc Hort Sci* **135**:83-89.

Werner AK and Witte C-P (2011) The biochemistry of nitrogen mobilization: purine ring catabolism. *Trends Plant Sci* **16**:381-387.

Wittstock U and Gershenzon J (2002) Constitutive plant toxins and their role in defense against herbivores and pathogens. *Curr Op Plant Biol* **5**:300-307.

Witzel K, Weidner A, Surabhi G-K, Börner A and Mock H-P (2009) Salt stress-induced alterations in the root proteome of barley genotypes with contrasting response towards salinity. *J Exp Bot* **60**:3545-3557.

Xi L, Xu K, Qiao Y, Qu S, Zhang Z and Dai W (2011) Differential expression of ferritin genes in response to abiotic stresses and hormones in pear (Pyrus pyrifolia). *Mol Biol Rep* **38**:4405-4413.

Yan S-P, Zhang Q-Y, Tang Z-C, Su W-A and Sun W-N (2006) Comparative Proteomic Analysis Provides New Insights into Chilling Stress Responses in Rice. *Mol Cell Proteomics* **5**:484-496.

Yan S, Tang Z, Su W and Sun W (2005) Proteomic analysis of salt stress-responsive proteins in rice root. *PROTEOMICS* **5**:235-244.

Yelenosky G and Guy CL (1977) Carbohydrate Accumulation in Leaves and Stems of 'Valencia' Orange at Progressively Colder Temperatures. *Bot Gaz* **138**:13-17.

Yotov WV, Moreau A and St-Arnaud R (1998) The Alpha Chain of the Nascent Polypeptide-Associated Complex Functions as a Transcriptional Coactivator. *Mol Cell Biol* **18**:1303-1311.

Zhang L, Si J, Zeng F and An L (2009) Molecular cloning and characterization of a ferritin gene upregulated by cold stress in Chorispora bungeana. *Biol Trace Elem Res* **128**:269-283.

Figure 1.Two-dimensional electrophoresis maps of total proteins from control epicarp. This image was acquired using a 610 nm filter, according to the emission wavelength of the dye used to label this sample. Proteins were separated over the pI range 4–7 in the first dimension and on 15% (w/v) SDS-polyacrylamide gels in the second dimension. Protein spots differentially expressed are indicated by the number that appears in Table 3. In red, proteins induced in FE or FE+7d; in yellow, proteins decreased in FE or FE+7d respect to control samples.

Figure 2. Quantification of acids, sugars, alcohols and other compounds in endocarp. Determinations of relative metabolite concentrations were carried out using pools of six independent samples. Variation of levels of metabolites are expressed as the relative response ratio with respect to the ribitol internal standard and normalized to the fresh weight (in grams) of the sample. For each metabolite, bars with the same letters are not significantly different ($P < 0.05$).

Figure 3. Quantification of acids, sugars, alcohols and other compounds in epicarp. See legend to figure 2 for details.

Figure 4. Phenylpropanoid and flavonoid relative quantification in epicarp. The compounds levels were expressed as the area (mAU) of the peak in the chromatogram by gram of fresh weight. Results represent the mean of at least two biological replicates (different pools) ± standard deviation. For each metabolite, bars with the same letters are not significantly different ($P < 0.05$).

Figure 5. Expression analysis of transcripts of enzymes involved in carbon metabolism in epicarp analyzed by QRT-PCR. Analyses were carried out on RNA isolated from epicarp of C, FE and FE+7d samples. The means of the results obtained, using three independent RNAs as a template, are shown. Each reaction was normalized using the Ct values corresponding to *C. sinensis* elongation factor 1 mRNA. Standard deviations are shown. For each transcript analyzed, bars with the same letters are not significantly different ($P < 0.05$).

Table 1. Sequences of the oligonucleotide primers used for real-time PCR.

Transcript	Forward primer	Reverse primer	Product
MDH	5'-TGTCGAAGACAATGCCCTCTG-3′	5'-GAAGACTCGACAAATCTTGCTG-3′	160bp
EM	5'-TCTCTCCAACCCAACCTCAC-3′	5'-CAGGGAAGATGTAAGCATTG-3′	161bp
PK	5'-GCCCCGGTGATGCTGTG-3′	5'-TTGCCCCTACTCCCTCTAAAAG-3′	123bp
PEPC	5'-CGCCTTGCAACACCAGAAATG-3′	5'-CCCCAAAGCCAAGCCACAC-3′	160bp
PEPCK	5'-TGGTGCTACAGGATGGCTC-3′	5'-CTTGTAAGCCTGCTTGTCTG-3′	238bp
LDH	5'-GCCTATGAGAAGGAAACCCTAGAG-3′	5'-GGGTGAATCTTTCTCTGATCTC-3′	155bp
PDC	5'-GTGTGATTGCTTGCATTGGTG-3′	5'-CATTTACCAGGCCAGTATAATCC-3′	186bp
ADH	5'-GTTTGGGGTTACCGAGTTTGTG-3′	5'-TTAAGCAGATTCATGGGATGAG-3′	228bp
PFP α	5'-AGCTTCTTCTTCAACCCGAGTCAG-3′	5'-GTGTCCAAGAACGTAGGCATAGTC-3	221bp
PFP β	5'-GAGAGGAGACATGGCAAGTTCAAG-3′	5'-ACCGAGTTCGAGGAGTAGTGTG-3′	192bp
SPOT 14	5'-TGACAAGTTCGCTGTTGGAA-3′	5'-GCACCACCACCAGTTGATATG-3′	159bp
SPOT 15	5'-TCCTTTACCTGCACAGTCCG-3′	5'-TTTGGATGAAGCAAGTCCGC-3′	144bp
SPOT 18	5'-CGCAGTGGTGAGACTGAAGA-3′	5'-TAAACTGCTTCAGCACCGAG-3′	155bp
SPOT 26	5'-CGTCACTTGGATTGGTAGGC-3′	5'-AGCAAAGAACAAACGAAAGCTG-3′	156bp
EF-1	5'-GATATGCCCCAGTGCTTGAC-3′	5'-CTTGGTGGGAATCATCTTAAC-3′	158bp

Table 2. Effect of frost exposure on the chemical parameters of internal quality in *Citrus sinensis* oranges.

The experiments were repeated at least three times in C, FE and FE+7d samples. Different letters indicate data significantly different at $P < 0.05$ (Bonferroni t-test or Tukey test).

	C	FE	FE±7d
Soluble solids (ºBrix)	11.6 ± 0.3	11.7 ± 0.4	12.1 ± 0.4
Titratable acidity (%)	2.17 ± 0.32	1.85 ± 0.35	2.26 ± 0.45
Maturity index	5.33 ± 0.91	6.30 ± 0.20	5.35 ± 0.52
Volatile compounds			
Acetaldehyde (ppm)	14 ± 2a	20 ± 3b	23 ± 1b
Ethanol (ppm)	50 ± 6a	71 ± 14a	142 ± 26b

Table 3. List of differentially expressed proteins in control (C) and frost-exposed (FE) fruit.

The data are grouped in different portions according to the tissue analyzed and the time after frost. The second column shows changes of spot abundance ratios: negative values, if protein levels decrease in FE fruit with respect to control, or positive values, in the opposite case. For each spot, the MASCOT score, the accession number, the protein annotation, the sequence coverage, the number of matched and fragmented peptides and finally the theoretical and experimental relative molecular mass (Mr) and isolectric point (pI) are indicated. When the search was carried out using the *Viridiplantae* ESTs database, the EST accession number and the E-value associated to the best matching protein obtained via BLASTx are also indicated.

Comparisons														
Spot No	Ratio	MASCOT Score	EST Acc. No translated ORF	Acc. No of homologous found in NCBInr	Protein annotation of homologous found in NCBInr [*organism*]	E-value	Coverage %	Matched Peptides	Fragmented Peptides	Theoretical		Observed	
										Mr	pI	Mr	pI
Endocarp Comparisons													
C vs. FE													
1	+ 1,96	325	CK936514	XP_002524839.1	carboxymethylenebutenolidase, putative [Ricinus communis]	1E-158	54	19	3	29.30	6.78	23.00	5.52
2	+ 1,69				not significant hit							35.00	5.85
3	+	96	EY776637	AAC24001.1	isoflavone reductase related protein [Pyrus communis]	3E-134	17	6	2	34.60	8.29	32.00	6.45
4	-				not significant hit							20.00	5.00
5	-	125	EY855516	XP_002526668	ferritin, plant, putative [Ricinus communis]	1E-85	37	14	2	35.28	9.32	22.00	5.10
C vs. FE+7d													
3	+	125	EY855516	XP_002526668	ferritin, plant, putative [Ricinus communis]	1E-85	37	14	2	35.28	9.32	22.00	5.10
7	+	188	CX053546	ABB29926.1	fructose-bisphosphate aldolase-like [Solanum tuberosum]	0	25	5	2	29.44	5.53	38.00	6.55
6	-	372	CX043835	XP_002531678	adenosine kinase, putative [Ricinus communis]	1E-145	36	8	3	31.95	5.82	38.00	5.45
8	-	188	FC914586	XP_003528346.1	PREDICTED: 3-isopropylmalate dehydratase small subunit-like [Glycine max]	3E-109	43	8	3	29.00	6.10	21.00	5.35
9	-				not significant hit							22.00	5.45
10	-	157	DN799352	XP_002266597.1	PREDICTED: nascent polypeptide-associated complex subunit alpha-like [Vitis vinifera]	7E-101	54	6	2	20.52	5.86	25.00	4.52
Epicarp Comparisons													
C vs. FE													
11	+ 1,69				not significant hit							20.00	4.95
12	+ 1,90	104	EY767425	NP_178022.1	NADH dehydrogenase [ubiquinone] iron-sulfur protein 8 [Arabidopsis thaliana]	5E-126	29	10	2	34.02	5.59	25.00	4.70
14	+ 2,65	201	DY285744	XP_002513353.1	phosphoglycerate kinase, putative [Ricinus communis]	0	38	14	2	47.73	10.13	39.00	5.50
16	+	111	FC920136	XP_002513634.1	NADH dehydrogenase, putative [Ricinus communis]	3.00E-94	39	9	1	23.14	4.73	22.00	4.65
17	+	96	EY795890	XP_002284300.2	PREDICTED: germin-like protein subfamily 1 member 14 [Vitis vinifera]	1.00E-50	19	4	1	31,40	9,76	27.00	5.40
18	+	139	CX070059	ADD12953.1	2-phospho-D-glycerate hydrolase [Citrus trifoliata]	0	54	11	1	29.42	5.06	47.00	5.50
19	+	177	gi|123325705		ATP synthase beta subunit (chloroplast) [Oxanthera neocaledonica]		39	13	4	49.69	5.22	55.00	5.00

20	+	119	FC871152	XP_002534347.1	rubisco subunit binding-protein alpha subunit, putative [Ricinus communis]	5.00E-173	36	8	4	28.35	5.19	65.00	4.60
21	+				not significant hit							100.00	6.65
13	- 1,9				not significant hit							38.00	5.60
15	-2.43	111	gi|285309969		aconitate hydratase 2 [Citrus clementina]		14	13	2	98.48	6.09	90.00	6.10
22	-	140	DT555230	XP_003564580.1	PREDICTED: heat shock cognate 70 kDa protein-like [Brachypodium distachyon]	0	50	14	1	30.50	8.44	24.00	5.00
23	-	200	DR403908	ABL60873.1	germin-like protein 4 [Vitis vinifera]	8.00E-73	44	6	1	21.75	7.04	25.00	4.85
34	-				not significant hit							38.00	5.60
C vs. FE+7d													
25	-				not significant hit							15.00	5.45
26	-	101	CK938777	XP_003638459.1	Progesterone 5-beta-reductase [Medicago truncatula]	4e-146	32	8	1	31.62	5.21	50.00	5.55
27	-	204	GT972532	YP_002720120.1	Ribulose-1,5-bisphosphate carboxylase/oxygenase large subunit [Jatropha curcas]	9.00E-159	67	16	2	24.27	9.32	55.00	6.00

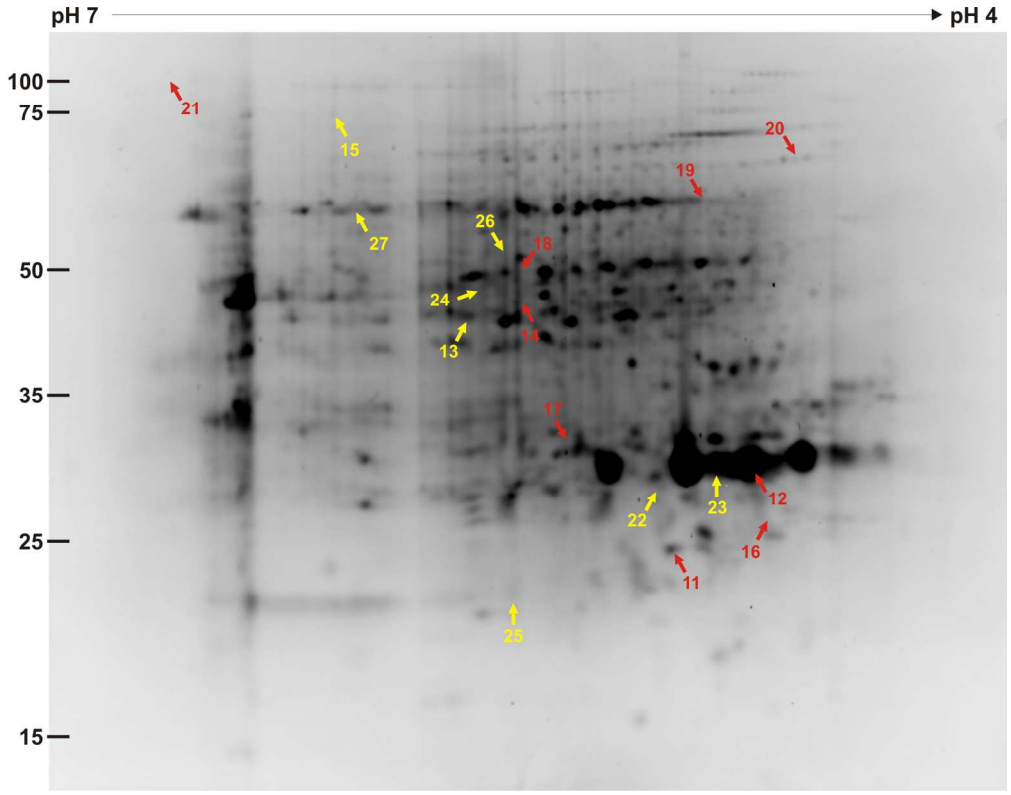

Figure 1.Two-dimensional electrophoresis maps of total proteins from control epicarp. This image was acquired using a 610 nm filter, according to the emission wavelength of the dye used to label this sample. Proteins were separated over the pI range 4–7 in the first dimension and on 15% (w/v) SDS-polyacrylamide gels in the second dimension. Protein spots differentially expressed are indicated by the number that appears in Table 3. In red, proteins induced in FE or FE+7d; in yellow, proteins decreased in FE or FE+7d respect to control samples.
159x124mm (300 x 300 DPI)

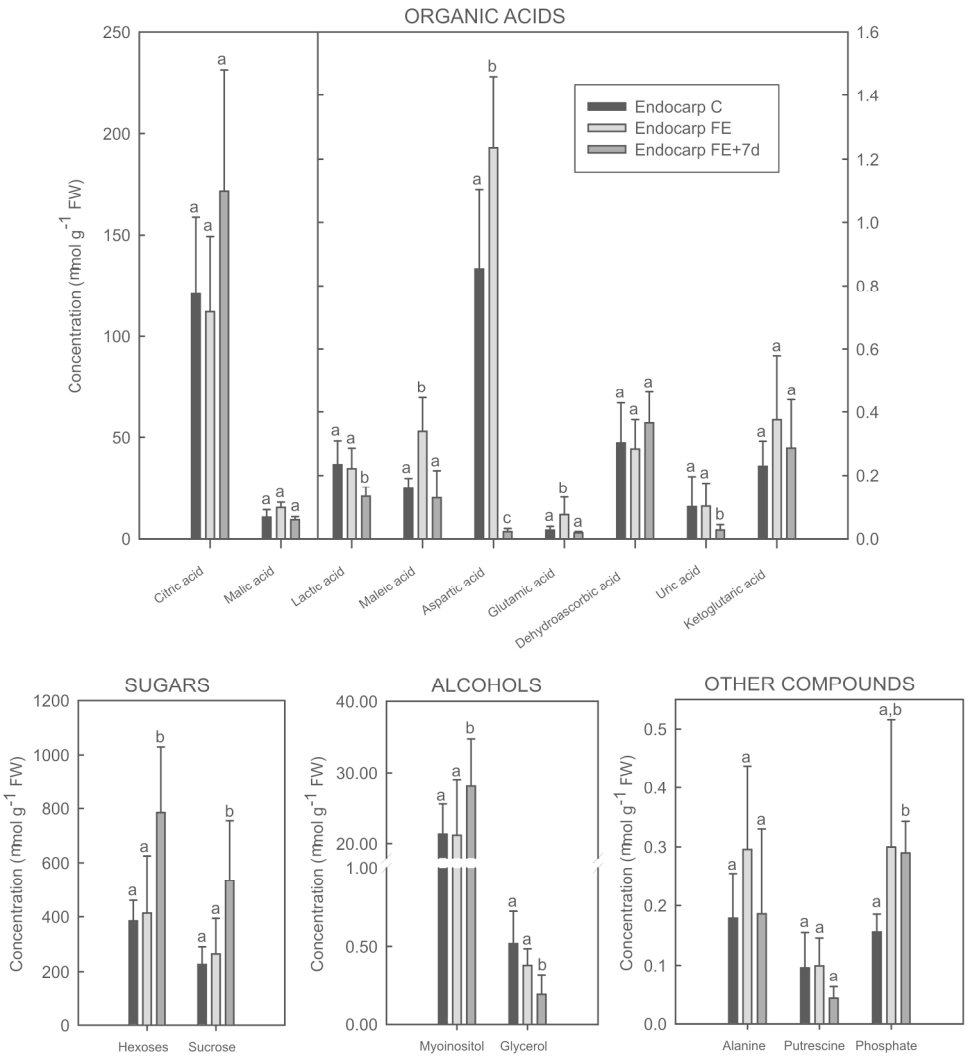

Figure 2. Quantification of acids, sugars, alcohols and other compounds in endocarp. Determinations of relative metabolite concentrations were carried out using pools of six independent samples. Variation of levels of metabolites are expressed as the relative response ratio with respect to the ribitol internal standard and normalized to the fresh weight (in grams) of the sample. For each metabolite, bars with the same letters are not significantly different ($P < 0.05$).
191x206mm (300 x 300 DPI)

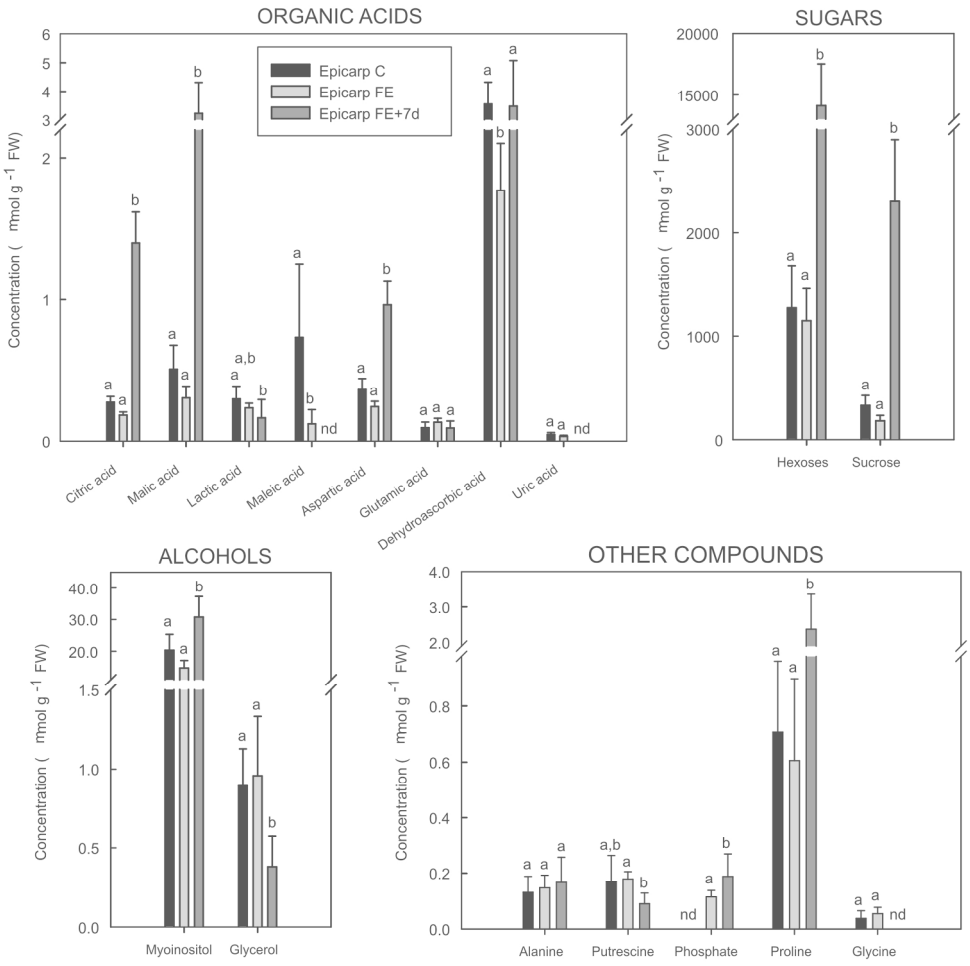

Figure 3. Quantification of acids, sugars, alcohols and other compounds in epicarp. See legend to figure 2 for details.
186x183mm (300 x 300 DPI)

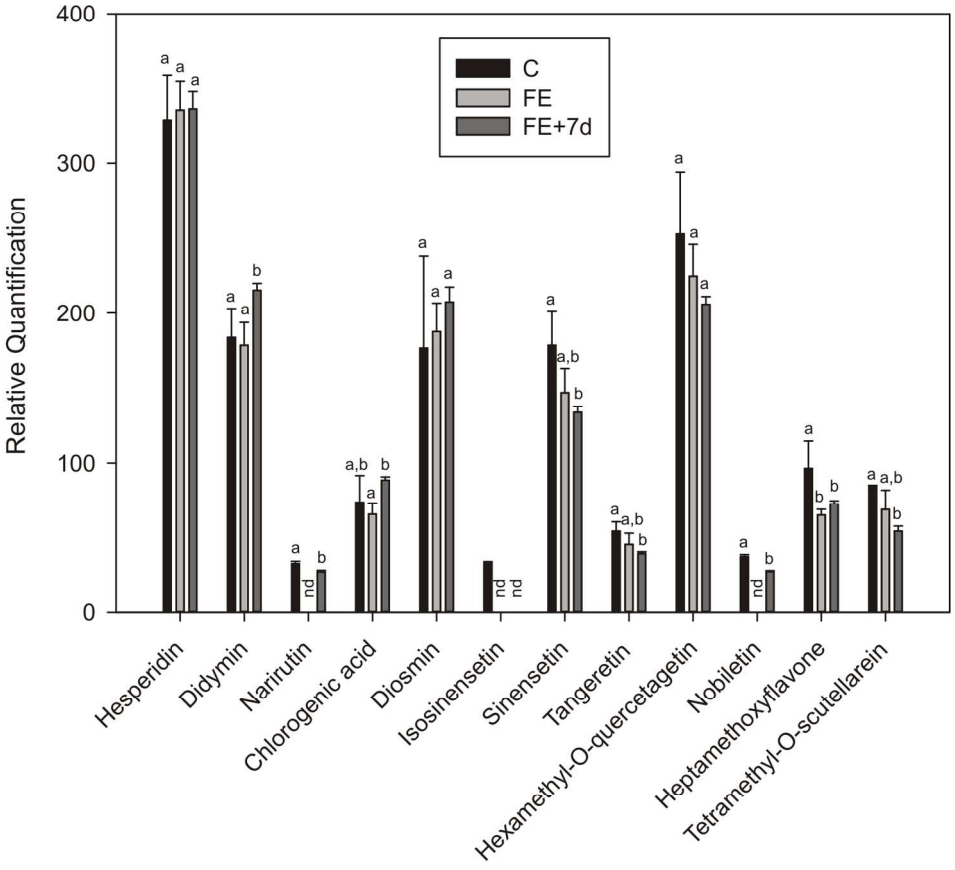

Figure 4. Phenylpropanoid and flavonoid relative quantification in epicarp. The compounds levels were expressed as the area (mAU) of the peak in the chromatogram by gram of fresh weight. Results represent the mean of at least two biological replicates (different pools) ± standard deviation. For each metabolite, bars with the same letters are not significantly different ($P < 0.05$).
150x145mm (300 x 300 DPI)

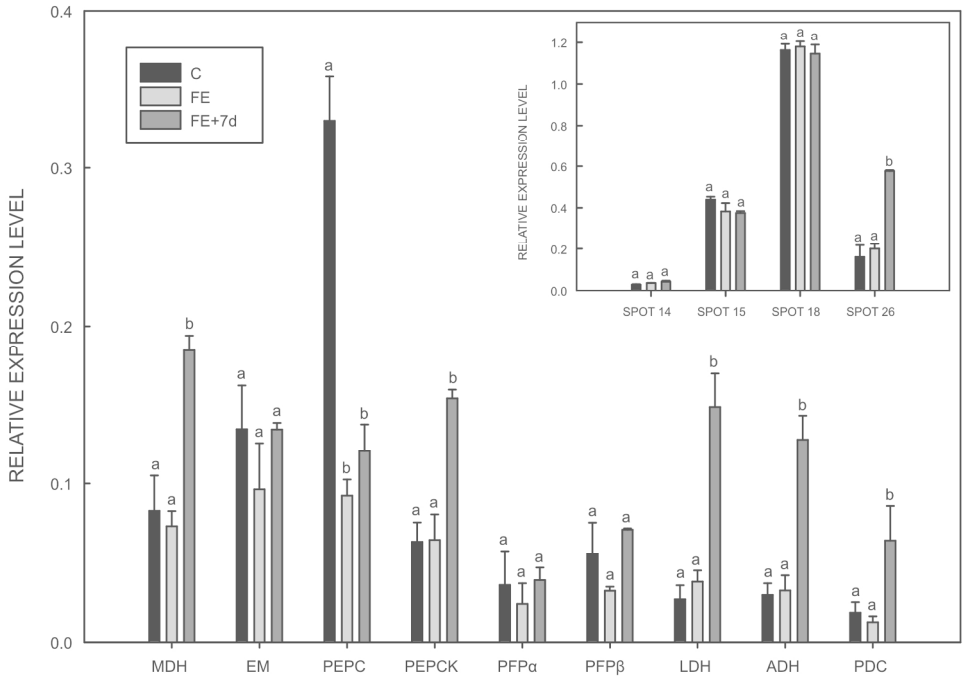

Figure 5. Expression analysis of transcripts of enzymes involved in carbon metabolism in epicarp analyzed by QRT-PCR. Analyses were carried out on RNA isolated from epicarp of C, FE and FE+7d samples. The means of the results obtained, using three independent RNAs as a template, are shown. Each reaction was normalized using the Ct values corresponding to C. sinensis elongation factor 1 mRNA. Standard deviations are shown. For each transcript analyzed, bars with the same letters are not significantly different ($P < 0.05$).
178x147mm (300 x 300 DPI)